ATMOSPHERIC SCIENCE LETTERS
Atmos. Sci. Let. **15**: 86–91 (2014)
Published online 17 October 2013 in Wiley Online Library
(wileyonlinelibrary.com) **DOI:** 10.1002/asl2.467

RMetS
Royal Meteorological Society

Decadal-scale variability in hazardous winds in northern Switzerland since end of the 19th century

Christoph Welker* and Olivia Martius

Oeschger Centre for Climate Change Research and Institute of Geography, University of Bern, Bern, Switzerland

*Correspondence to:
C. Welker, Institute of Geography, University of Bern, Hallerstrasse 12, Bern 3012, Switzerland.
E-mail:
christoph.welker@giub.unibe.ch

Received: 21 May 2013
Revised: 10 September 2013
Accepted: 11 September 2013

Abstract

The decadal-scale variability in winter hazardous winds in northern Switzerland from 1871 to present is investigated in the Twentieth Century Reanalysis (20CR). Independent wind speed measurements taken at Zurich climate station show that the interannual and decadal variability in hazardous winds in northern Switzerland is realistically represented in the 20CR. Both time series exhibit pronounced decadal-scale variability with periods between approximately 36 and 47 years. At these periodicities, the hazardous wind variability in northern Switzerland is positively correlated with the variability in the North Atlantic Oscillation, however the strength and statistical significance of their co-variability varies over time.

Keywords: hazardous winds in Switzerland; decadal-scale variability; NAO; quality assessment of 20CR

1. Introduction

Strong winter storms are among the most damaging and expensive meteorological hazards in Switzerland and their decadal-scale variations are of considerable interest since low frequency variability is crucial for the statistical analysis of extremes (Katz, 2010). The scarce availability of long-term atmospheric data series has so far limited the quantitative analysis of decadal-scale changes of winter storms over Switzerland. On the basis of qualitative historic wind speed estimates and measurements taken at four meteorological measuring stations in northern Switzerland, Schiesser *et al.* (1997) analyzed long-term trends in the number of winter storm days and found that the period between the mid-1860s and 1940 contained more winter storm days than the period afterwards. Furthermore, Wang *et al.* (2011) estimated geostrophic wind speeds over Europe using historic surface pressure observations and showed that in the Alpine region the frequency of strong geostrophic wind events in winter has increased notably from the mid to the late 20th century. In general, geostrophic wind speeds over Central Europe in the past approximately 130 years exhibited pronounced decadal-scale variability and were loosely correlated with the North Atlantic Oscillation (NAO) (Matulla *et al.*, 2008).

Recently, the novel Twentieth Century Reanalysis (20CR) data set (Compo *et al.*, 2011) has been used to assess low frequency changes in windstorms over Europe and over other parts of the world (Donat *et al.*, 2011b; Brönnimann *et al.*, 2012; Wang *et al.*, 2012). However, currently it is controversial whether 20CR can be used to assess decadal climate variability. Krueger *et al.* (2013a, 2013b) found considerable disagreement between Northeast Atlantic storminess derived from 20CR and from observations, in particular prior to 1950, and they question the applicability of the 20CR data set for the assessment of decadal-scale changes of windstorms in this region. This has been challenged by Wang *et al.* (2013) who found that the storminess in the North Atlantic and European region derived from the 20CR and from observations are in good agreement back to approximately 1893 with some disagreement before then. Furthermore, a qualitative comparison of historic wind speed measurements from Zurich and the 20CR shows generally a good agreement (Brönnimann *et al.*, 2012).

The main objectives of this article are twofold (1) to analyze the decadal-scale variability in hazardous winds in northern Switzerland for the extended winter season December through March (DJFM) using wind data from 20CR and observations and (2) to extend the work by Brönnimann *et al.* (2012) and to provide a quantitative assessment of the agreement between 20CR wind data and the observation-based data set.

2. Data and methods

We use version 2 of the 20CR, a global atmospheric reanalysis with 2-degree spatial and 6-hourly temporal resolution spanning 1871 to present (Compo *et al.*, 2011). Only surface pressure observations were assimilated into the 20CR data set. An Ensemble Kalman Filter assimilation technique was applied to create an ensemble of 56 members. Monthly sea surface temperature (SST) and sea ice distributions from the Hadley Centre Sea Ice and SST (HadISST) data set (Rayner *et al.*, 2003) served as boundary conditions. Refer

Compo *et al.*'s (2011) study for further details on the 20CR data set.

To quantify the loss potential associated with high winds we calculate the cubes of the wind speeds exceeding the local annual 98th percentiles of wind speed. This measure is henceforth referred to as wind loss potential (WLP). This is motivated by the empirical findings that the monetary loss through windstorms rises roughly with the cube of the wind speed (Emanuel, 2005) and that the local 98th percentile is a loss-relevant threshold (refer Klawa and Ulbrich, 2003; Donat *et al.*, 2011a; Pinto *et al.*, 2012 for more details).

We compute the WLP for each ensemble member using near-surface wind speeds (0.995-sigma; ca. 30–40 m above ground) from 20CR in 1871–2008. The winter WLP at each grid cell i is calculated by summing the cubes of the 6-hourly wind speeds V_j exceeding the loss-relevant local 98th percentile of wind speed V_{p98}:

$$\mathrm{WLP\,(season)}_i \equiv \sum_{j=1}^{n} \left(V_{i,j} \geq V_{p98,i}\right)^3$$

The 98th percentile corresponds to the wind speed that is exceeded on average on 7 days per year. We determine the local annual 98th percentiles for each 20CR ensemble member using 6-hourly near-surface wind speed data for the whole 138-year period available. The ensemble averages of these local 98th percentiles of wind speed are then used in the computation of the WLP for the 20CR Switzerland grid cells. We define the 20CR Switzerland grid cells as the domain 6°E–10°E, 46°N–48°N. This includes Switzerland and parts of the neighboring countries. In the coarse resolution topography of the 20CR these grid cells are either located on the Alpine north side or in the Alps (Figure S1). The complex topography of Switzerland is not realistically represented in the 20CR (Stucki *et al.*, 2012). This has important ramifications for the representation of local wind systems in Switzerland like Föhn winds that are strongly influenced by the local topography.

The 20CR near-surface winds are compared to independent, homogenized daily maxima of hourly wind speed measurements taken at Zurich climate station (Usbeck *et al.*, 2010). These data are available for the extended winter seasons DJFM from 1891 to today. For this time series the 94th percentile of wind speed is used as threshold for the computation of the WLP for Zurich. The seasonal 94th percentile is chosen because the number of selected high wind events (7 days per DJFM) roughly corresponds to the annual 98th percentile (7 days per year) under the assumption that all high wind events occur during the extended winter season DJFM. In the 20CR data set, approximately two thirds of all WLP events (i.e. WLP values at 6-h intervals greater than 0 $m^3\ s^{-3}$) for Switzerland from 1871 to 2008 occurred during this season.

The station-based DJFM NAO index (based on Hurrell, 1995) is used to determine the decadal-scale NAO variability and its relation to the WLP variability in northern Switzerland.

We use a wavelet analysis technique to identify the dominant modes of variability in both the WLP and the NAO time series. These analyses follow Torrence and Compo (1998) and Grinsted *et al.* (2004) and we use their wavelet softwares. The Morlet wavelet function is used for the computation of the continuous wavelet transforms (CWTs; Torrence and Compo, 1998). The region of the CWT power spectrum where edge effects become important is called cone of influence (COI). We test the statistical significance of wavelet power against the null hypothesis that the signal is produced by a stationary process with a given mean power spectrum (Grinsted *et al.*, 2004). We assume that the time series are approximately normally distributed with red noise characteristics that can be modeled with a first order autoregressive process. To examine whether two time series are linked, we compute the cross wavelet transform (XWT) and the wavelet coherence (WTC) from their CWTs (Grinsted *et al.*, 2004). Following Grinsted *et al.* (2004), the statistical significance of the WTC is calculated using a Monte Carlo method.

3. Results

First, the interannual variability in the winter WLP for Switzerland derived from 20CR and independent wind observations in Zurich are compared (Figure 1(a) and (b)). For the overlapping time period from 1892 to 2008 the Pearson correlation coefficients between the 20CR and the observed time series range from 0.69 to 0.72 for the individual ensemble members. The median of the ensemble distribution is 0.71. These correlations are quite high, however, some differences between the 20CR and observed time series are apparent in the relative amplitude of the WLP of individual winters. This is a consequence of the comparison of wind information aggregated over a domain of $6^\circ \times 4^\circ$ with a point measurement in Zurich, where local effects like the Föhn wind system can be responsible for high wind events (Brönnimann *et al.*, 2012). These local effects cannot be captured in the 20CR due to the coarse spatial resolution of the topography of the Alps in this data set.

Encouragingly, the 20CR ensemble range of the winter WLP for the Switzerland grid cells, which is a measure of the uncertainty, is small compared to the interannual and decadal-scale variability and the data set is hence suited for analyzing decadal-scale changes (Figure 1(b)).

To analyze the decadal winter WLP variability quantitatively, we apply a wavelet analysis technique. First, the CWT power spectrum of the standardized (i.e. in units of standard deviation with zero mean) 20CR ensemble mean winter WLP is computed

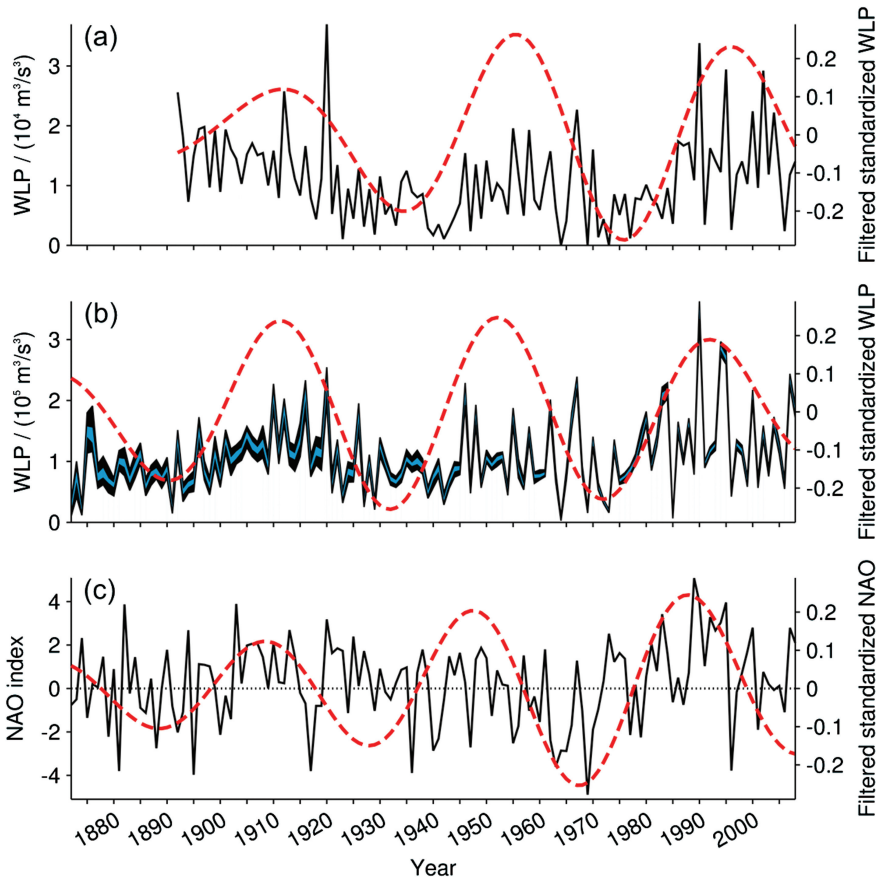

Figure 1. (a) DJFM WLP for Zurich (1892–2008) based on instrumental wind speed measurements. (b) 20CR DJFM WLP for the Switzerland grid boxes (1872–2008). The 20CR ensemble distribution is shown: the black (cyan) area indicates the ensemble range (interquartile range). Note the different ranges of the left *y*-axes in panels (a) and (b). (c) Station-based DJFM NAO index (1872–2008). The thick dashed red curves indicate the corresponding 36–47-year wavelet-filtered standardized time series (right *y*-axes). At the beginning and end of the time period the amplitude of the wavelet-filtered time series has been reduced due to zero padding before doing the CWT (refer Torrence and Compo, 1998 for details).

(Figure 2(b)). This time series shows statistically significant wavelet power at low frequencies, namely at periods between about 36 and 47 years. However, due to the limited length of the time series, these results are partly inside the COI. The time series of the observed winter WLP for Zurich shows statistically significant wavelet power in the same oscillation band (Figure 2(a)). In general, the CWT power spectra derived from the 20CR (Figure 2(b)) and observations (Figure 2(a)) agree very well, not only on decadal but also on interannual time scales for the overlapping period 1892–2008. This is confirmed both by the XWT, which describes the common power of the two CWTs and their phase relationship (Figure 2(c)), and by the squared WTC (Figure 2(d)), which roughly corresponds to the local correlation between the two CWTs. In the time periods with statistically significant, high common power at interannual and decadal time scales in the CWTs, the phase relationship between the 20CR WLP and the observed WLP is mostly in-phase (Figure 2(c)). The squared WTC is high and statistically significant at periodicities of 36–47 years (Figure 2(d)). Furthermore, we use the wavelet transform as a bandpass filter (refer Torrence and Compo, 1998 for details) to isolate the 36–47-year variability in the time series of the standardized 20CR ensemble mean winter WLP for the Switzerland grid cells and of the standardized observed winter WLP for Zurich (dashed curves in Figure 1(a) and (b)). These filtered time series are highly correlated.

The decadal-scale winter WLP variability in northern Switzerland was potentially associated with large scale atmospheric and oceanic low frequency variability in the North Atlantic basin, such as the Atlantic Multidecadal Oscillation (AMO) or the NAO. The winter AMO and the 20CR winter WLP for northern Switzerland have no co-variability at periodicities of 36–47 years (Figure S2). The WLP and the station-based winter NAO index have common power and a constant phase relationship in the decadal oscillation range (Figure 3(b)), with the NAO variability leading the WLP variability by approximately 5 years (refer also Figure 1(b) and (c)). However, the common wavelet power signal is only statistically significant between approximately the 1920s and the 2000s. In this time period (and in particular toward the end of this period), the CWT power spectrum of the winter NAO index shows high, but not statistically significant power at periodicities of 36–47 years and weaker power before then (see Figures 1(c) and 3(a)). The

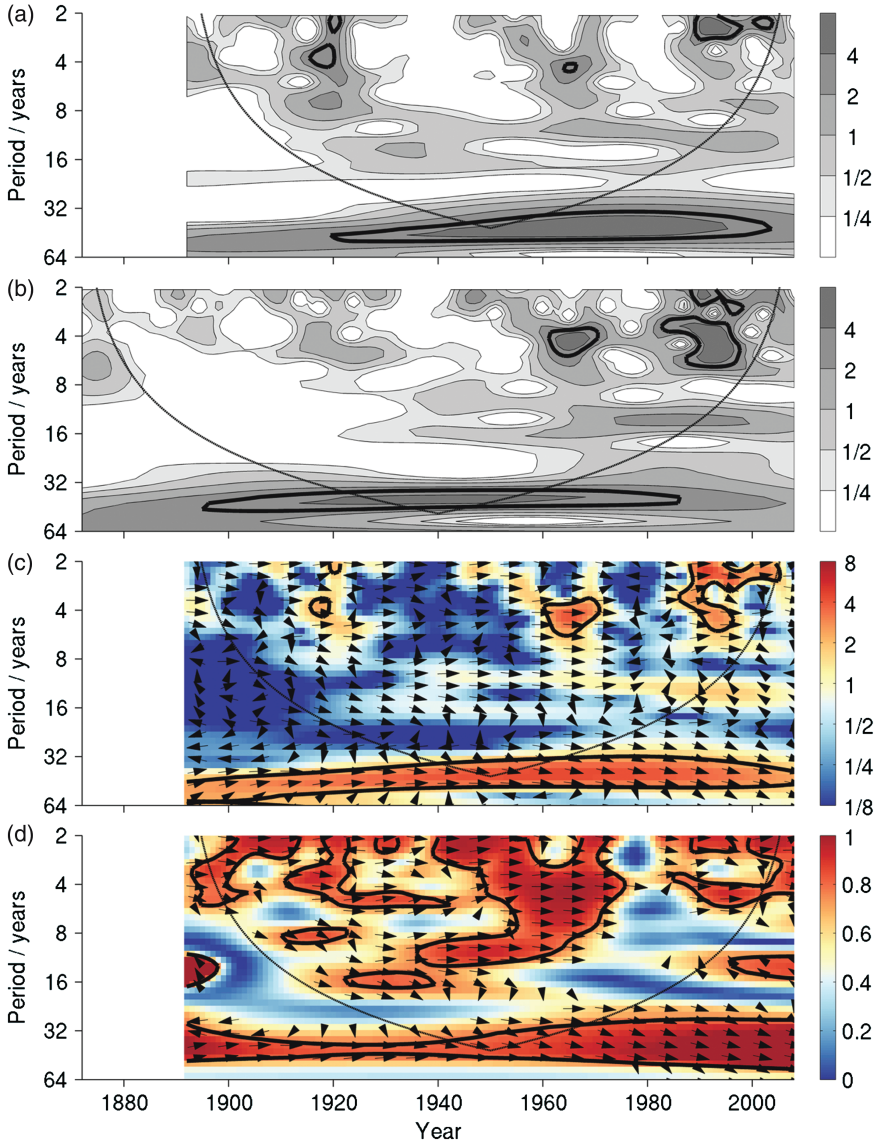

Figure 2. CWT power spectra of the standardized (a) observed DJFM WLP for Zurich and (b) 20CR ensemble mean DJFM WLP for the Switzerland grid cells from 1892 (or 1872, respectively) to 2008. The abscissa indicates the time (year) and the ordinate is the Fourier period (in years). The thick black contour lines show the 5-% significance level. The thin black line denotes the COI where edge effects become important. (c) XWT and (d) squared WTC computed from the CWTs in panels (a) and (b) for 1892–2008. The arrows in panels (c) and (d) are the same and indicate the relative phase relationship: in-phase pointing right, out-of-phase pointing left.

correlation (i.e. the squared WTC) between the 20CR winter WLP for the Switzerland grid cells and the winter NAO index time series is high and statistically significant in the decadal oscillation range (Figure 3(c)).

4. Summary and conclusions

The decadal-scale variability in winter season hazardous wind speeds in northern Switzerland since the end of the 19th century is investigated. We use a simple index to quantify the local WLP of windstorms and apply this index to the 20CR ensemble data set and to historic instrumental wind speed observations taken at Zurich climate station. The main focus is on Switzerland, where the ensemble uncertainty of 20CR is small compared to the decadal variability. This allows for analyzing decadal-scale winter WLP changes.

The WLP of winter storms over northern Switzerland since end of the 19th century exhibited pronounced decadal-scale variability with periods between approximately 36–47 years. The decadal variability in the winter WLP for the Switzerland grid cells derived from the 20CR is confirmed by independent wind measurements taken in Zurich. We find a statistically significant agreement between the 20CR WLP and observations not only on decadal but also on interannual time scales.

The 20CR wind records span only 138 years and it remains open whether the decadal-scale variability with a period of approximately 40 years is a truly oscillatory phenomenon. Answering this question will

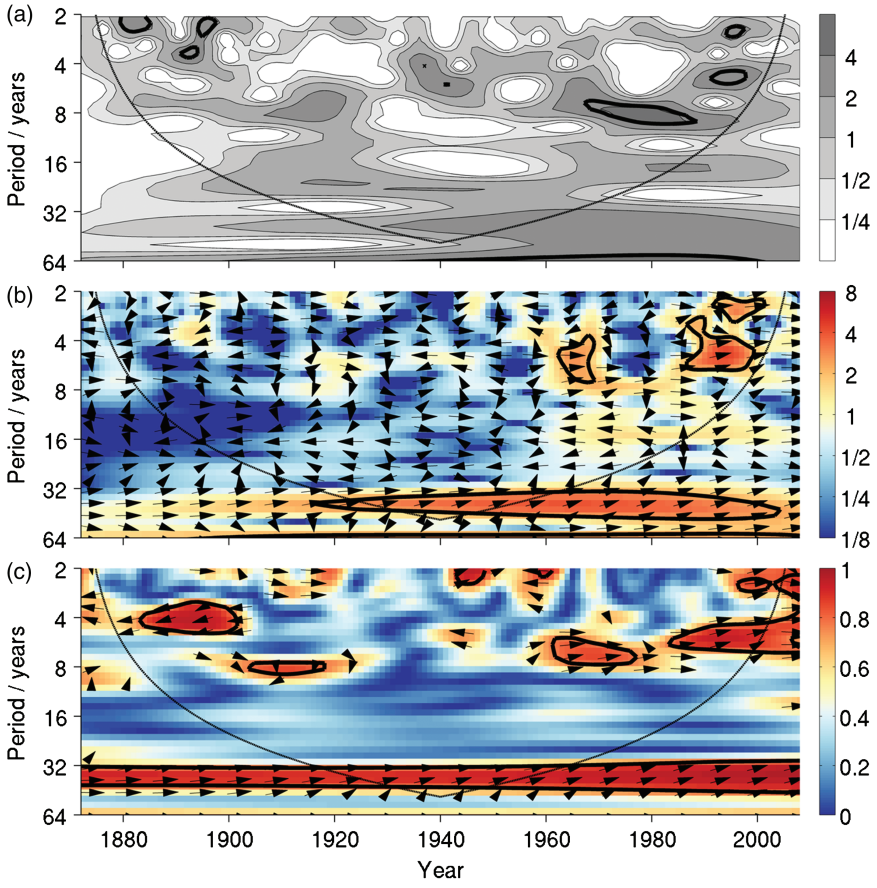

Figure 3. (a) CWT power spectrum of the standardized station-based DJFM NAO index in 1872–2008. (b) XWT and (c) squared WTC between the DJFM NAO index and the 20CR ensemble mean DJFM WLP for the Switzerland grid cells.

require longer time series and a detailed understanding of the underlying processes. First analyses indicate that while the NAO is important for the variability of windstorms in northern Europe (Matulla *et al.*, 2008; Donat *et al.*, 2010), this link is less distinct for the winter WLP variability in northern Switzerland. The decadal-scale variability in the 20CR winter WLP is positively correlated with the corresponding decadal winter NAO variability. However, the common wavelet power of the two time series in the decadal-scale oscillation range varies over time and is only statistically significant between approximately the 1920s and the 2000s. An interesting aspect of the co-variability of the two time series is a constant phase shift of approximately 5 years, with the NAO leading the WLP. Understanding the reasons for this lag will require more detailed analyses that include the potentially important role of the ocean.

Supporting information

The following supporting information is available:

Figure S1. The color shade indicates the 20CR orography (i.e. geopotential height at surface) for Switzerland and parts of the neighboring countries. The 2-min gridded ETOPO2v2 relief data serves to show the location of mountainous regions exceeding 1000 m a.s.l. (black contour lines). In addition, this data set is used to derive sea areas (light blue areas). The 20CR Switzerland grid cells (6°E–10°E, 46°N–48°N) are framed by a dashed blue box. The border of Switzerland is plotted in white. The location of Zurich (8.6°E, 47.4°N; ca. 400 m a.s.l.) in northern Switzerland is marked with a red star.

Figure S2. Analogous to Figure 3 in the article, however instead of the station-based DJFM NAO index the mean DJFM AMO index (unsmoothed; Enfield *et al.*, 2001) is used.

Appendix S1. Evaluation how representative the WLP for Zurich is compared to the WLP for other parts of Switzerland.

Acknowledgements

We thank two anonymous reviewers for comments that substantially improved the quality of the manuscript. We thank T. Usbeck for providing historic instrumental wind speed data taken at Zurich climate station and S. Brönnimann for useful comments. Support for the Twentieth Century Reanalysis Project data set is provided by the US Department of Energy, Office of Science Innovative and Novel Computational Impact on Theory and Experiment (DOE INCITE) program, and Office of Biological and Environmental Research (BER), and by the National Oceanic and Atmospheric Administration Climate Program Office. Hurrell's NAO index record is retrieved from http://climatedataguide.ucar.edu/guidance/hurrell-north-atlantic-oscillation-nao-index-station-based (last access: July 2013). Wavelet software is available from http://atoc.colorado.edu/research/wavelets/ and http://www.pol.ac.uk/

home/research/waveletcoherence/ (last access to the web pages: March 2012).

References

Brönnimann S, Martius O, von Waldow H, Welker C, Luterbacher J, Compo GP, Sardeshmukh PD, Usbeck T. 2012. Extreme winds at northern mid-latitudes since 1871. *Meteorologische Zeitschrift* **21**: 13–27.

Compo GP, Whitaker JS, Sardeshmukh PD, Matsui N, Allan RJ, Yin X, Gleason BE, Vose RS, Rutledge G, Bessemoulin P, Brönnimann S, Brunet M, Crouthamel RI, Grant AN, Groisman PY, Jones PD, Kruk MC, Kruger AC, Marshall GJ, Maugeri M, Mok HY, Nordli Ø, Ross TF, Trigo RM, Wang XL, Woodruff SD, Worley SJ. 2011. The Twentieth Century Reanalysis project. *Quarterly Journal of the Royal Meteorological Society* **4**: 1–28.

Donat MG, Leckebusch GC, Pinto JG, Ulbrich U. 2010. Examination of wind storms over Central Europe with respect to circulation weather types and NAO phases. *International Journal of Climatology* **30**: 1289–1300.

Donat MG, Leckebusch GC, Wild S, Ulbrich U. 2011a. Future changes in European winter storm losses and extreme wind speeds inferred from GCM and RCM multi-model simulations. *Natural Hazards and Earth System Sciences* **11**: 1351–1370.

Donat MG, Renggli D, Wild S, Alexander LV, Leckebusch GC, Ulbrich U. 2011b. Reanalysis suggests long-term upward trends in European storminess since 1871. *Geophysical Research Letters* **38**: L14703, DOI: 10.1029/2011GL047995.

Emanuel K. 2005. Increasing destructiveness of tropical cyclones over the past 30 years. *Nature* **436**: 686–688.

Grinsted A, Moore JC, Jevrejeva S. 2004. Application of the cross wavelet transform and wavelet coherence to geophysical time series. *Nonlinear Processes in Geophysics* **11**: 561–566.

Hurrell JW. 1995. Decadal trends in the North Atlantic Oscillation: regional temperatures and precipitation. *Science* **269**: 676–679.

Katz RW. 2010. Statistics of extremes in climate change. *Climatic Change* **100**: 71–76.

Klawa M, Ulbrich U. 2003. A model for the estimation of storm losses and the identification of severe winter storms in Germany. *Natural Hazards and Earth System Sciences* **3**: 725–732.

Krueger O, Schenk F, Feser F, Weisse R. 2013a. Inconsistencies between long-term trends in storminess derived from the 20CR reanalysis and observations. *Journal of Climate* **26**: 868–874.

Krueger O, Feser F, Bärring L, Kaas E, Schmith T, Tuomenvirta H, von Storch H. 2013b. Comment on "Trends and low frequency variability of extra-tropical cyclone activity in the ensemble of twentieth century reanalysis" by Xiaolan L. Wang, Y. Feng, G. P. Compo, V. R. Swail, F. W. Zwiers, R. J. Allan, and P. D. Sardeshmukh. Climate Dynamics, 2012. *Climate Dynamics*, DOI: 10.1007/s00382-013-1814-9.

Matulla C, Schöner W, Alexandersson H, von Storch H, Wang XL. 2008. European storminess: late nineteenth century to present. *Climate Dynamics* **31**: 125–130.

Pinto JG, Karremann MK, Born K, Della-Marta PM, Klawa M. 2012. Loss potentials associated with European windstorms under future climate conditions. *Climate Research* **54**: 1–20.

Rayner NA, Parker DE, Horton EB, Folland CK, Alexander LV, Rowell DP, Kent EC, Kaplan A. 2003. Global analyses of sea surface temperature, sea ice, and night marine air temperature since the late nineteenth century. *Journal of Geophysical Research* **108**: 4407, DOI: 10.1029/2002JD002670.

Schiesser HH, Pfister C, Bader J. 1997. Winter storms in Switzerland north of the Alps 1864/1865-1993/1994. *Theoretical and Applied Climatology* **58**: 1–19.

Stucki P, Rickli R, Brönnimann S, Martius O, Wanner H, Grebner D, Luterbacher J. 2012. Weather patterns and hydro-climatological precursors of extreme floods in Switzerland since 1868. *Meteorologische Zeitschrift* **21**: 531–550.

Torrence C, Compo GP. 1998. A practical guide to wavelet analysis. *Bulletin of the American Meteorological Society* **79**: 61–78.

Usbeck T, Wohlgemuth T, Pfister C, Volz R, Beniston M, Dobbertin M. 2010. Wind speed measurements and forest damage in Canton Zurich (Central Europe) from 1891 to winter 2007. *International Journal of Climatology* **30**: 347–358.

Wang XL, Wan H, Zwiers FW, Swail VR, Compo GP, Allan RJ, Vose RS, Jourdain S, Yin X. 2011. Trends and low-frequency variability of storminess over western Europe, 1878-2007. *Climate Dynamics* **37**: 2355–2371.

Wang XL, Feng Y, Compo GP, Swail VR, Zwiers FW, Allan RJ, Sardeshmukh PD. 2012. Trends and low frequency variability of extra-tropical cyclone activity in the ensemble of twentieth century reanalysis. *Climate Dynamics* **40**: 2775–2800.

Wang XL, Feng Y, Compo GP, Zwiers FW, Allan RJ, Swail VR, Sardeshmukh PD. 2013. Is the storminess in the Twentieth Century Reanalysis really inconsistent with observations? A reply to the comment by Krueger *et al.* (2013b). *Climate Dynamics*, DOI: 10.1007/s00382-013-1828-3.

